




Virus Quantification Methods with Focus on Marek's Disease Viruses



Mohammad Reza Piriaei¹, Jamshid Razmyar¹, Sara Dolatyabi², Mohammad Hasan Bozorgmehrfard^{1*}

¹ Department of Avian Diseases, Faculty of Veterinary Medicine, University of Tehran, Tehran, Iran

² Department of Animal Sciences, Ohio State University, Ohio, United State of America

* Corresponding author email address: mhbfard@yahoo.com

Article Info

Article type:

Review Article

How to cite this article:

Piriaei, M. R., Razmyar, J., Dolatyabi, S., & Bozorgmehrfard, M. H. (2023). Virus Quantification Methods with Focus on Marek's Disease Viruses. *Journal of Poultry Sciences and Avian Diseases*, 1(1), 40-51.

<http://dx.doi.org/10.61838/kman.jpsad.1.1.5>



© 2023 the authors. Published by SANA AVIAN HOSPITAL, Tehran, Iran. This is an open access article under the terms of the Creative Commons Attribution 4.0 International (CC BY 4.0) License.

ABSTRACT

Marek's disease (MD) is a significant concern in the poultry industry, causing neoplastic disease and substantial economic losses. MDV-1, MDV-2, and MDV-3 are the three serotypes of the herpesvirus that cause MD, each with unique traits and interactions with the host. Vaccination is the primary preventive measure, but some vaccinated flocks still experience losses, often due to suboptimal vaccine dosages. Accurate quantification of the virus is crucial for understanding its dynamics, evaluating vaccine efficacy, and ensuring the health and productivity of poultry populations. Virus quantification methods fall into two main categories: infectivity assays and chemical/physical assays. Infectivity assays detect active, infectious virions, such as plaque, focus formation, and endpoint dilution. Chemical/physical assays, including the hemagglutination assay, transmission electron microscopy, flow cytometry, and qPCR, target specific components of the virion. However, these methods cannot distinguish between infectious and inactivated virions, potentially leading to overestimating viable viral populations. Marek's disease viruses (MDVs) can be quantified using in vitro plaque assays in susceptible cell cultures. The viral plaque assay determines the number of plaque-forming units (pfu) in a virus sample. Titration procedures for vaccine strains are similar to those for pathogenic variants. It is crucial to assess the dose of reconstituted MD vaccine (in PFU per chicken) to identify potential vaccine inefficacies and prevent outbreaks in the field. Accurate virus quantification is pivotal in understanding viral kinetics, optimizing therapeutic interventions, evaluating vaccine effectiveness, and preventing Marek's disease outbreaks in poultry.

Keywords: Marek's disease, Cell culture, Viral particles, Virus quantification assays

1 Introduction

Marek's disease (MD) is a highly contagious viral neoplastic condition affecting chickens. The disease is attributed to an alpha herpesvirus, which is classified into three distinct serotypes (1). Characteristically, like other herpesviruses, this virus exhibits strict cell association (2).

Serotype 1 (GaHV-2) encompasses oncogenic Marek's disease viruses, exhibiting a spectrum of pathogenicities ranging from mildly virulent to very virulent plus. In contrast, Serotype 2 (GaHV-3) is characterized by apathogenic viruses derived from chickens, while Serotype 3 is identified as a non-oncogenic turkey herpesvirus, also known as MeHV-1 (1, 3).

Article history:

Received 26 December 2022

Accepted 08 February 2023

Revised 13 February 2023

Published Online 01 March 2023

The disease was initially delineated by Jozsef Marek as a polyneuritis (1, 4) Subsequent research illuminated the multifaceted nature of the virus, revealing its association with a variety of syndromes Notably (3), MD holds the distinction of being the first oncogenic disease effectively managed through vaccination (2). As such, its prevention hinges on a combination of vaccination and rigorous biosecurity measures. Globally, a vaccination regimen is universally adopted for parent stock and layers. In several countries, including the United States, routine MD vaccination is a standard practice for commercial broilers. Prior to the advent of vaccination, MD exerted a significant economic toll on the poultry sector, with mortality rates in layer farms reaching alarming highs of around 60% in certain instances. Additionally, MD accounted for nearly 10% of condemnations in broiler farms (1). The integration of MD vaccines in broiler chicken management has markedly enhanced flock performance, primarily through the mitigation of mortality and morbidity rates (5).

Vaccines spanning all serotypes have been developed to combat MD (3) The CVI-988 strain stands out as one of the most widely adopted MD vaccines globally (6, 7). This strain, a mildly virulent serotype 1 isolate, is renowned for its superior protective efficacy (8, 9). Additionally, SB-1 and 301B/1, both derived from serotype 2, are prominent in bivalent and polyvalent vaccine formulations. The Herpes Virus of Turkey (HVT/FC-126), also known as MeHV-1, is benign in both chickens and turkeys. However, it can induce viremia, which subsequently triggers protective immunity (10).

The twin pillars of MD vaccines are immunity and safety. Predominantly, these vaccines are formulated from live virus strains, necessitating multiple passages for their transformation into viable vaccines—particularly for oncogenic serotype 1 strains. The passage count is contingent on the specific virus strain. Even with the appropriate attenuation for vaccine production, challenges persist in ensuring vaccine efficacy. A suboptimal viral particle count in a vaccine dose can compromise its immunogenicity, leading to inadequate protection (11) As evidenced in some instances, this shortfall can result in MD outbreaks even in vaccinated flocks (1, 12). Conversely, an excessively high viral particle count can jeopardize vaccine safety. Thus, precise determination of the viral particle count in vaccine doses is imperative (12). This article will delve into the diverse methodologies available for virus quantification.

2 Virus Quantification Methods

Viral quantification methodologies can be broadly categorized into two primary types: infectivity assays and chemical/physical assays. Infectivity assays quantify virions by assessing their capability to invade cells and generate infectious offspring. Notably, these assays exclude inactivated (non-infectious) virions from their count. On the other hand, chemical/physical assays focus on the identification of specific virion components, such as unique viral proteins or the viral genome. However, these techniques do not differentiate between infectious and inactivated virions (13).

2.1 Infectivity Assays

2.1.1 Plaque Assay

Plaque-based assays are foundational techniques in virology, employed extensively to ascertain the infectious dose in viral concentrations. These assays quantify the plaque-forming units (pfu) within a virus sample, offering a reliable metric for viral load. The methodology hinges on a microbiological process executed in petri dishes or multi-well plates. Here, a host cell monolayer is exposed to varying viral concentrations. Subsequently, a semi-solid overlay, typically agar or carboxymethyl cellulose, is applied to curtail the uncontrolled diffusion of the viral infection. As the virus invades a cell within this monolayer, it initiates the formation of a viral plaque (14). This infection triggers a cascade: the infected cell undergoes lysis, releasing the virus to infect adjacent cells, perpetuating the infection-to-lysis cycle. The resultant plaque, essentially a zone of infection surrounded by uninfected cells (refer to Figure 1), becomes discernible either under an optical microscope or to the naked eye. Visualization is enhanced by introducing a crystal violet solution, which stains the cytoplasm, leaving the lysed cells unstained and thus highlighting the plaque's location (15).

The duration for plaque formation can span 3–14 days, contingent on the virus under scrutiny. Typically, plaques are enumerated manually, and factoring in the dilution used, this data facilitates the computation of pfu per unit volume (pfu/mL). This metric, pfu/mL, serves as an indicator of the infectious particle concentration within the sample. It operates on the premise that each plaque is indicative of a singular infectious virus particle For a majority of animal viruses, a linear relationship exists between the count of infectious particles (16, 17). and the plaque tally. However,

a limitation of this technique is its specificity: it can only evaluate viruses that induce discernible cytological alterations in cultured cells (18)

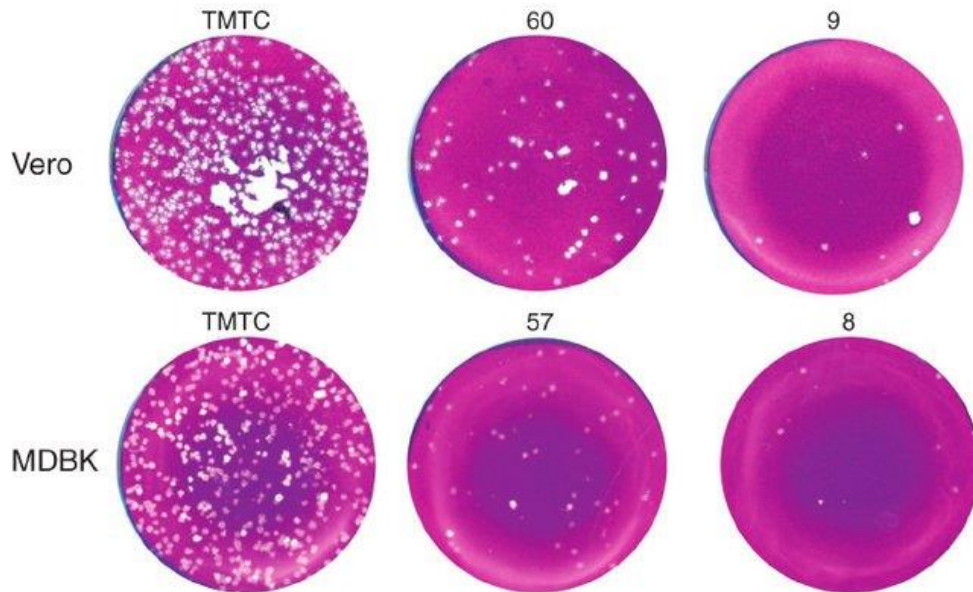


Figure 1. Plaque assay in Vero (upper panel) and MDBK (lower panel) cells with Herpes Simplex Virus Type 1 (HSV-1)

2.1.2 Focus Forming Assay (FFA)

The focus forming assay (FFA) stands as a nuanced adaptation of the traditional plaque assay, leveraging immunostaining techniques for plaque detection rather than relying on cell lysis. Central to this method is the use of fluorescently labeled antibodies tailored to a specific viral antigen, facilitating the identification of both infected host cells and infectious viral particles (19). This assay proves particularly advantageous for assessing virus types that don't induce cell membrane lysis, as such viruses remain undetected in conventional plaque assays (20).

In the FFA procedure, host cell monolayers are exposed to varying concentrations of the viral sample. Following infection, a brief incubation period ensues (typically spanning 24–72 hours) under an overlay of agar or another semi-solid medium. This overlay curtails the unbridled spread of the infectious virus, leading to the formation of localized clusters or 'foci' of infected cells. Subsequent stages involve probing these plates with the aforementioned fluorescent antibodies targeting a viral antigen. Fluorescence microscopy then aids in enumerating the foci (21).

One of the FFA's salient advantages is its expedited result generation, outpacing other assays like the plaque or fifty-percent-tissue-culture-infective-dose (TCID-50) tests. However, this speed comes at a cost, with the requisite

reagents and equipment often bearing a steeper price tag. The assay's duration is also influenced by the counting area's size: larger areas necessitate more time but yield a more accurate representation of the sample. Results from the FFA are typically articulated as focus forming units per milliliter (FFU/ml) (20).

2.1.3 Endpoint Dilution Assay

The Endpoint dilution assay, a venerable method predating the plaque assay, remains a staple in virological titration. This assay involves inoculating serial dilutions of a virus into cultures, eggs, or animals. Its primary objective is to ascertain the quantity of the virus required to either kill 50% of the infected hosts or induce a cytopathic effect in half of the inoculated tissue culture cells. It becomes particularly pertinent in clinical research scenarios when determining a virus's fatal dose or when dealing with viruses that don't form plaques.

In a tissue culture setting, this assay is often denoted as TCID-50. However, when animals are the subjects, the results might be expressed as Infectious Dose 50% (ID-50) or Lethal Dose 50% (LD-50) (20, 22). The assay's duration can extend to a week, attributed to the time required for cell infection (23). A notable characteristic of this method is the relative nature of the declared viral titers; they aren't absolute

and are influenced by the specific cells or animals employed in the assay (24).

Two prevalent computational methods associated with endpoint dilution assays (encompassing TCID-50, EC-50, IC-50, and LD-50) are:"

-Spearman-Karber method:

$$\log_{10} 50\% \text{ end point dilution} = - (x_0 - d/2 + d \sum r_i/n_i)$$

x_0 = log₁₀ of the reciprocal of the highest dilution (lowest concentration) at which all animals are positive; d = log₁₀ of the dilution factor; n_i = number of animals used in each individual dilution (after discounting accidental deaths); r_i = number of positive animals (out of n_i). Summation is started at dilution x_0 [25].

-Reed-Muench method:

$\log_{10} 50\% \text{ end point dilution} = \log_{10}$ of dilution showing a mortality next above 50% - (difference of logarithms \times logarithm of dilution factor)

Mainly, this formula is used for calculation of "difference of logarithms" (which is also known as "proportionate distance" or "interpolated value").

Difference of logarithms = [(mortality at dilution next above 50%)-50%]/[(mortality next above 50%)- (mortality next below 50%)].

The relationship between TCID-50 and PFU, grounded in theoretical constructs, suggests that 0.69 PFU is approximately equivalent to 1 TCID-50. This relationship is derived from the Poisson distribution (23), a statistical model that predicts the likelihood of a given number of random events (in this case, virus particles) occurring within a fixed interval, given a known average rate of occurrence (here, the virus titer). This distribution is particularly apt for scenarios where events are rare, such as the probability of a virus particle being present in a specific volume of medium in a well. From a mathematical perspective, the anticipated PFUs would exceed half the TCID-50 value. This is because the negative tubes in the TCID-50 assay correspond to zero plaque forming units, while the positive tubes can represent one or multiple plaque forming units. For a more nuanced and accurate estimate, the Poisson distribution serves as an invaluable tool (25).

2.2 Chemical and Physical Assays

2.2.1 Hemagglutination Assay

"The hemagglutination assay (HA) stands as a widely recognized non-fluorescence protein estimation technique. Notably, viruses from the Adenoviridae, Orthomyxoviridae, and Paramyxoviridae families possess proteins capable of

binding to erythrocytes. In the HA procedure, two-fold dilutions of the virus are combined with a specific quantity of red blood cells. Following a designated incubation period, agglutinated red blood cells create a diffuse lattice pattern, while unagglutinated cells settle into a button-like formation. The assay yields results in hemagglutination units (HAU), with the typical pfu to HAU ratios hovering around the 10⁶ range (25-27). While the HA method boasts speed and cost-effectiveness, its outcomes can be significantly influenced by the user's technical expertise (28). A notable limitation of HA is its inability to differentiate between viable and inactivated viruses within a sample (23, 29).

Building on the foundational HA assay, the hemagglutination inhibition assay (HI) emerges as a pivotal variant, primarily employed to gauge antibody concentrations in blood serum. This is especially relevant for pathogens like influenza and Newcastle disease viruses (30). The crux of the HI assay lies in the interference it introduces between serum antibodies targeting the virus and the virus's ability to bind to red blood cells. Consequently, when antibody concentrations reach a critical threshold, they inhibit hemagglutination (31-34).

2.2.2 Bicinchoninic Acid Assay

The bicinchoninic acid assay (BCA) operates on a fundamental colorimetric principle. The stock BSA solution comprises key components such as Bicinchoninic acid, Sodium carbonate, Sodium bicarbonate, sodium tartrate, and Copper (II) sulfate pentahydrate (35). A hallmark of this assay is the transition of the stock solution's color from green to purple, indicative of the total protein concentration (30). This colorimetric shift unfolds in two distinct phases. Initially, peptide bonds present in viral proteins catalyze the reduction of Cu²⁺ to Cu⁺. Subsequently, BCA chelates the Cu⁺ ions in a 2:1 stoichiometric ratio, culminating in the characteristic purple hue that exhibits peak absorbance at 562 nm (36). This absorbance serves as a metric to ascertain the overarching protein concentration within the sample. Post-assay, the results are juxtaposed against established standard curves, facilitated by spectrophotometric or plate reader analyses. The assay's duration is relatively brief, ranging from 30 minutes to an hour. While the BCA assay is lauded for its speed and broad applicability, it grapples with specificity challenges, given its propensity to detect all protein entities. As such, it's imperative that viral preparations are minimally contaminated with host cell proteins to ensure accuracy (37).

2.2.3 Single Radial Immunodiffusion Assay

The Single Radial Immunodiffusion assay (SRID), colloquially termed the Mancini method, stands as a specialized protein assay tailored to quantify specific viral antigens through immunodiffusion in a medium, which can be liquid or semi-solid like agar (34, 38). This medium is imbued with an antigen-specific antiserum, and the target antigen is strategically placed at the disc's epicenter. As the antigen diffuses outward into the medium, it instigates the formation of a precipitate ring, which continues to expand until an equilibrium state is achieved (39).

The assay's duration is inherently variable, spanning anywhere from a mere 10 hours to several days, contingent on the equilibration dynamics between the antigen and antibody. A salient feature of this assay is the linear relationship between the precipitate ring's diameter and the logarithm of the protein's concentration. For quantification purposes, this diameter is benchmarked against established standards corresponding to certified protein concentrations (40).

While SRID remains in active use, it's not without its constraints. The assay is notably time-intensive and grapples with accuracy challenges, often exhibiting coefficients of variation (CV) exceeding 10%. Its sensitivity is another concern; SRID typically struggles to quantify sample concentrations below 4 µg/mL. Furthermore, the assay's outcomes are influenced by the quantity and structural configuration of the antigen (39, 40).

2.2.4 Transmission Electron Microscopy (TEM)

The Transmission Electron Microscopy (TEM) technique harnesses a beam of electrons, which, when focused using a magnetic field, enables imaging of a sample. A significant advantage of TEM over traditional light microscopy is its superior spatial resolution, offering up to a thousand-fold enhancement (with resolutions reaching 0.2 nm) (41). For effective imaging, the specimen must be ultrathin and undergo negative staining. During sample preparations, specimens are deposited onto a TEM-specific coated grid and subsequently stained with an electron-opaque substance. Additionally (42), thinly sectioned tissue-embedded samples can be assessed using TEM. While sample preparation protocols can vary based on the operator and specific methodology, the process typically spans several hours (43).

TEM's prowess lies in its ability to visualize individual viral particles (44). For quantifying virus concentrations, one can employ quantitative image analysis (as depicted in Figure 1). Beyond mere quantification, the high-resolution images furnished by TEM offer invaluable insights into particle morphology, a feat unattainable by most alternative techniques (45). It's noteworthy that quantitative TEM results tend to surpass those from other assays, given its capacity to quantify all particles, regardless of their infectivity. Consequently, results are presented as virus-like particles per mL (vlp/mL) (46). In terms of operational parameters, quantitative TEM is optimally suited for virus concentrations exceeding 10^6 particles/ml (43, 47).

However, TEM's adoption is somewhat restricted due to its substantial equipment costs, spatial requirements, and the need for specialized support facilities, making it exclusive to certain well-equipped institutions (44).

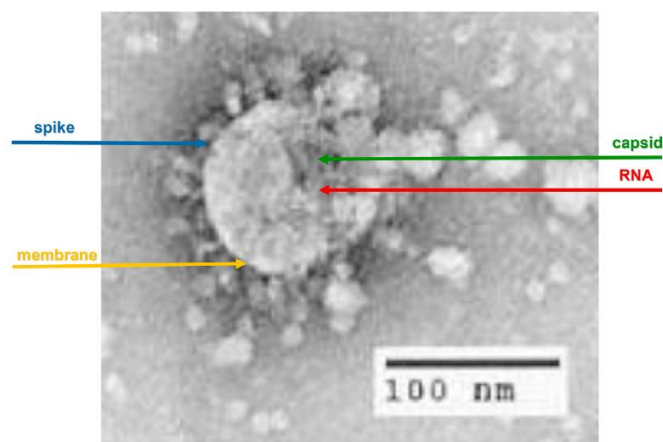


Figure 2. Negative stain electron microscopy of SARS-COV 2 showing spike, membrane, capsid and RNA genome

2.2.5 Tunable resistive pulse sensing (TRPS)

Tunable Resistive Pulse Sensing (TRPS) emerges as a cutting-edge technique, facilitating high-throughput assessments of individual virus particles as they traverse a size-adjustable nanopore, one at a time (48). Notably, this method offers the dual capability of gauging both the size and concentration of virus particles within a sample with remarkable precision. Such measurements prove instrumental in evaluating sample stability, discerning the influence of aggregates, and quantifying the overall concentration of viral particles (vp/mL) (49).

An inherent advantage of TRPS is its operation within an ionic buffer, obviating the need for pre-staining of samples. Consequently, this technique surpasses others that necessitate preliminary treatment with fluorescent dyes in terms of speed and efficiency (50). The entire process, encompassing sample preparation and measurement, is accomplished in under 10 minutes per sample, rendering it notably expeditious.

Commercially, TRPS-based virus analysis is readily accessible through platforms like the qViro-X systems. Furthermore, these systems can be effectively decontaminated through chemical autoclaving post-measurement (51).

2.2.6 Flow Cytometry

Traditionally, flow cytometers were employed for the detection of cells, cell populations, and surface antigens on cells (52). However, the evolving landscape of flow cytometry science in recent years has expanded its capabilities to encompass the detection of microparticles, falling within the size range of 100 nm to 1000 nm (53). These microparticles may constitute cellular components, such as exosomes (54) or even smaller entities like bacteria and viruses (55). The term 'flow virometry' aptly characterizes the application of a flow cytometer for the detection of viral particles (56).

It's important to note that there are limited commercially available flow cytometers suitable for quantifying viruses, primarily due to the stringent sensitivity requirements (57). A specialized apparatus, known as a 'virus counter,' assumes the role of quantifying intact viral particles within a sample through a process reliant on fluorescence-based identification of co-localized proteins and nucleic acids. The sample is stained with two distinct dyes—one specific to proteins and the other to nucleic acids—and is subsequently

analyzed as it flows through a laser beam. The count of particles generating coincident events on each of the two separate fluorescence channels, coupled with the measured sample flow rate, furnishes the virus particle concentration (vp/mL). Typically, the results align closely with those obtained from Transmission Electron Microscopy (TEM), providing absolute quantification. This assay operates effectively within a linear working range spanning 10^5 to 10^9 vp/mL, and the entire analysis can be completed in approximately 10 minutes, with minimal sample preparation time (58).

2.2.7 Single Virus Inductively Coupled Plasma Mass Spectroscopy (SV ICP-MS)

This technique bears resemblance to the Single Particle Inductively Coupled Plasma Mass Spectroscopy (SP ICP-MS), which was initially pioneered by Degueldre and Favarger in 2003 (59). Subsequently, in 2006, it was adapted for the analysis of various nanoparticles (60). In the ensuing research endeavors, it became evident that with certain methodological adaptations, this technology could be harnessed for the detection and quantification of viruses, leading to the emergence of Single Virus ICP-MS (SV ICP-MS) (61, 62).

In SV ICP-MS, following the atomization and ionization processes within the plasma torch, a burst of ions traverses through a conical pinhole and is subjected to scrutiny by a mass spectrometer. The quantity of these ion bursts corresponds directly to the number of viruses present within the sample, while the intensity is proportional to the fraction of isotope ions. The primary ions constituting a virus comprise elements found in its membrane, lipid layers, S-proteins, capsid, and nucleic core, including hydrogen (H), carbon (C), nitrogen (N), and oxygen (O) isotopes. Commonly detected ion isotopes by the ICP-MS mass spectrometer include $^{12}\text{C}^+$, $^{13}\text{C}^+$, $^{14}\text{N}^+$, and $^{15}\text{N}^+$ (63).

One of the remarkable capabilities of SV ICP-MS is its ability to routinely analyze single viruses, capturing mass spectrometry peaks over a time scan for specific masses and detecting a range of 2 to 500 viruses within a mere 20 seconds. In contrast, other techniques, such as electron microscopy, demand significantly more time for virus quantification, making SV ICP-MS several thousand times faster (64).

2.2.8 *Quantitative Polymerase Chain Reaction (qPCR)*

Quantitative Polymerase Chain Reaction (qPCR) harnesses the power of the polymerase chain reaction to amplify viral DNA or RNA, achieving concentrations that are amenable to detection and quantification through fluorescence-based assays (65). Typically, quantification relies on the use of serial dilutions of standards with known concentrations, which are analyzed alongside the unknown samples. These standards serve as calibration and reference points for accurate quantification.

In quantitative detection, a diverse array of fluorescence detection strategies can be employed, including sequence-specific probes and non-specific fluorescent dyes like SYBR Green (66). Sequence-specific probes, such as TaqMan (developed by Applied Biosystems), Molecular Beacons, or Scorpion probes, selectively bind to DNA sequences synthesized during the reaction, ensuring specificity. In contrast, SYBR Green dye attaches to all double-stranded DNA generated during the reaction (67). Although SYBR Green is straightforward to use, its lack of specificity and lower sensitivity have prompted many laboratories to opt for probe-based qPCR detection schemes (68, 69).

The qPCR process encompasses several variations, including the comparative threshold method, which enables relative quantification by comparing Ct values (PCR cycles indicating statistically significant increases in the product) from multiple samples that include an internal standard (69).

It's worth noting that PCR amplifies all target nucleic acids, including those originating from intact infectious virus particles, defective viral particles, and free nucleic acids in the solution (70). Consequently, the ratio of whole virions to copies of nucleic acid is seldom one-to-one for virus quantification (genome copies/mL). This discrepancy arises from variations in nucleic acid and viral protein production during viral replication, as well as the viral assembly process, which yields complete virions alongside

empty capsids and/or excess free viral genomes. The advantages of titration by qPCR are its rapid turnaround time (typically 1–4 hours) and high sensitivity, making it capable of detecting viruses at significantly lower concentrations than other methods (71).

2.2.9 *Enzyme-Linked Immunosorbent Assay (ELISA)*

Enzyme-Linked Immunosorbent Assay (ELISA) stands as a contemporary and versatile protein assay designed for the detection and quantification of specific substances, typically antigens, within a given sample (72, 73). ELISA capitalizes on the specificity of antibodies by employing an antibody that is conjugated to an enzyme. The antigen of interest is immobilized, either directly or through a specific antibody, within the assay (74).

The crux of ELISA lies in its capacity to detect and quantify the antibody-antigen binding event through the enzyme's catalytic activity. This catalysis results in the conversion of a reagent into a discernible signal, which can be harnessed to estimate the concentration of the antigen (as illustrated in Figure 3) (74-76). Horseradish peroxidase (HRP) is a commonly used enzyme in ELISA setups due to its ability to amplify signals and enhance assay sensitivity (31). ELISA assays come in various types, with the primary categories being direct (where the primary detection antibody is directly labeled with an enzyme), indirect (involving a secondary detection antibody), competitive, sandwich, or reverse configurations (31, 33, 74, 76).

Commercially available ELISA kits are offered by numerous companies, and quantification primarily relies on chromogenic reporters or fluorescence (76). ELISA is renowned for its sensitivity, specificity, and rapid turnaround time (77). It's important to note, however, that ELISA exclusively detects viral antigens and does not ascertain the presence of infectious viruses

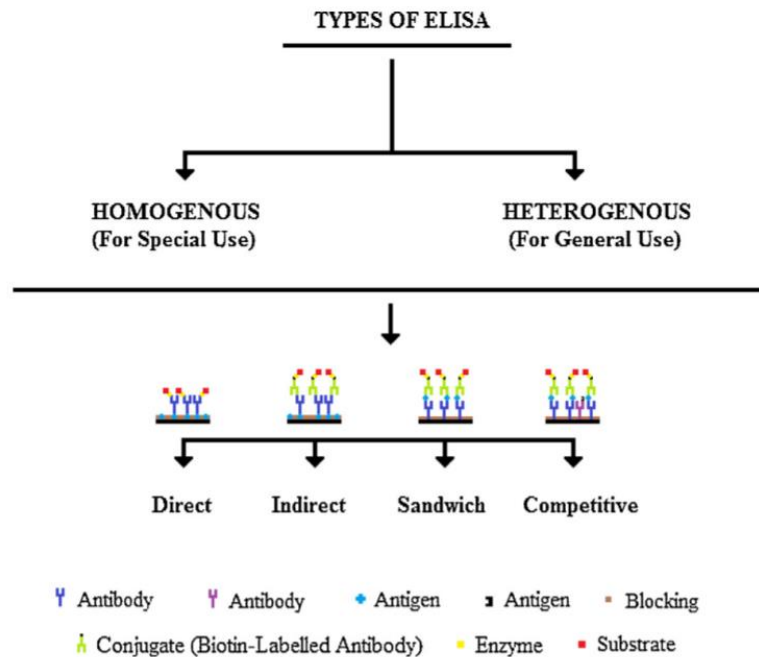


Figure 3. types of ELISA

3 Marek's Disease Virus Assay and Titration

The primary diagnostic methods employed for detecting Marek's disease include virus isolation, antigen detection, and the assessment of antibodies against Marek's disease virus (MDV) using Enzyme-Linked Immunosorbent Assay (ELISA) and the Agar Gel Immunodiffusion (AGID) assay (77). For all three serotypes of MDV, *in vitro* techniques have been established, with each serotype demanding specific approaches (77, 78). Broadly speaking, these techniques fall into two distinct categories for virus titration, primarily differentiated by their principles of quantification. Infectivity assays are based on the virus's ability to infect host cells and are generally considered more reliable than chemical or physical assays (79).

As previously elucidated, two prominent methods for virus quantification, namely plaque assays and focus forming assays, have demonstrated minimal differences in their results. For the primary isolation of MDV, a common approach involves inoculating susceptible cell cultures with blood lymphocytes or single-cell suspensions obtained from lymphoid tissues of infected chickens. The choice of cell substrate for primary isolation depends on the serotype of MDV in question. Chicken kidney cells and Duck Embryo

Fibroblast (DEF) cultures are preferred substrates for serotype 1 of MDV, while Chicken Embryo Fibroblast (CEF) cultures are generally used for isolating viruses of serotypes 2 and 3, as well as attenuated serotype 1 vaccine strains. It is important to note that CEF may not support the growth of low passage serotype 1 viruses as effectively, but contemporary isolates may perform well in CEF, even during primary isolation. Typically, cultures are inoculated with $1-2 \times 10^6$ cells, as doses exceeding 8×10^6 cells may inhibit viral plaque formation for certain viruses (80).

Isolation of MDV is confirmed by the development of characteristic plaques (as depicted in Figure 4) in inoculated cultures within 3-12 days, while comparable uninoculated or sham-inoculated control cultures should exhibit no such changes. Plaques induced by serotype 1, 2, and 3 viruses can be distinguished by morphological characteristics with practice, although a more precise differentiation is achieved through Immunofluorescence (IF) staining with serotype-specific monoclonal antibodies. The optimal time for plaque observation may vary depending on the cell substrate and the virus's serotype. Additionally, MDV can be isolated by directly culturing kidney cells obtained from infected chickens or by inoculating normal kidney cultures with trypsinized kidney cells from infected chickens (5).

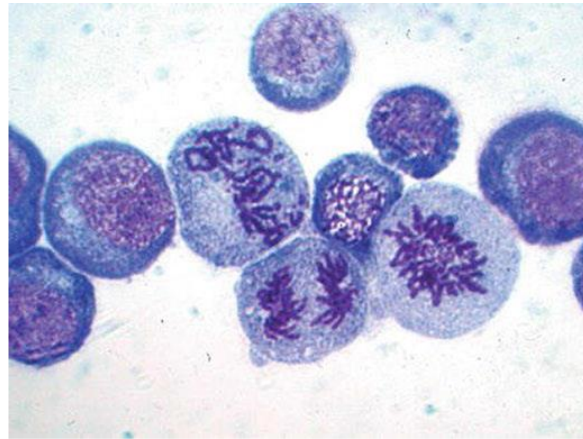


Figure 4. Smear from the MDCC-RP1 cell line. Note the characteristic lymphoblastoid morphology and the mitotic figures. Giemsa, $\times 1500$.

Enumeration should be done as soon as plaques become mature (time varies with isolate), because secondary plaques may occur when cultures are maintained with liquid medium. Procedures for titration of vaccine viruses have been reviewed in (13) and are not fundamentally different from those for pathogenic isolates (81).

4 Titration of Vaccines

Titration of Marek's disease (MD) vaccines is commonly carried out using the plaque assay method (82). It is imperative that this titration process is not restricted to evaluating the vaccine directly from the vial but also extends to assessing the reconstituted vaccine. However, conducting plaque assays for reconstituted vaccines can be challenging, as it necessitates access to cell culture facilities, which are typically not available at hatcheries. Key insights into vaccine titrations are conveniently summarized in Table 1. An alternative approach for evaluating vaccine quality at the hatchery involves assessing live cell counts. Although this method does not directly provide information about the quantity of vaccine virus present, it can serve as an indirect indicator of suboptimal management. If the number of dead cells is exceptionally high or if it rapidly increases following reconstitution, it may signal issues with vaccine handling and administration.

Table 1. Important facts on vaccine titrations.

It gives the number of PFU per administered dose.
It should be done from resuspended vaccine.
Vaccines are cell suspensions and there is variability of doses within a vial (range of doses)
Vaccine titration should be done in replicates (10-20 replicates)
Results can vary from laboratory to laboratory depending on cell culture protocols
It should be done in laboratories with experience in Marek's disease cell culture

A comprehensive investigation was conducted in the Netherlands, encompassing five distinct hatcheries, with the primary aim of scrutinizing the occurrence of authentic vaccine failures. The investigation employed *in vitro* assays to quantify the plaque-forming units (PFU) of Marek's disease (MD) vaccine per chicken dose. This evaluation was carried out on both vaccine vials, where 2 to 5 vials were sampled from each hatchery, and on samples of reconstituted vaccine, amounting to approximately 22 samples from each hatchery.

The findings were rather revealing. In hatcheries 1 and 4, it was observed that all forty reconstituted vaccine samples exhibited PFU counts falling below the crucial threshold of 103. Notably, hatchery 4 was of particular concern, as it had 14 samples with alarmingly low PFU counts, measuring equal to or less than 10 PFU. In contrast, hatcheries 2, 3, and 5 demonstrated a more favorable outcome, with only a small fraction of MD vaccine suspensions meeting the requisite standard of having a titer of at least 103 PFU. Specifically, hatchery 2 had 1 sample (5%), hatchery 3 had 17 samples (77%), and hatchery 5 had 3 samples (14%) meeting this stipulated criterion. Additionally, it was noted that some vaccine ampoules contained exactly 103 PFU per chicken dose. The implications of this study are substantial. It underscores the critical importance of diligently assessing the PFU per chicken dose for both reconstituted MD vaccine and vaccine vials. Such assessments are pivotal for the early detection of genuine vaccine failures, as their oversight could potentially culminate in disease outbreaks within poultry populations.

Conflict of Interest

The authors declared no conflicts of interest.

Authors Contributions

All authors have contributed in writing, critically reviewed, and approved final version of the manuscript.

Data Availability Statement

Data are available from the first author upon reasonable request.

References

1. McMullin PF. Diseases of poultry 14th edition: David E. Swayne, Martine Boulianne, Catherine M. Logue, Larry R. McDougald, Venugopal Nair, David L. Suarez, Sjaak de Wit, Tom Grimes, Deirdre Johnson, Michelle Kromm, Teguh Yodiantara Prajitno, Ian Rubinoff & Guillermo Zavala (Eds.), Hoboken, NJ, John Wiley & Sons, 2020, 1451 pp.,£ 190 (hardcover)/£ 171.99 (e-book), ISBN 9781119371168. Taylor & Francis; 2020. <https://doi.org/10.1080/03079457.2020.1794237>
2. Boodhoo N, Gurung A, Sharif S, Behboudi S. Marek's disease in chickens: a review with focus on immunology. *Veterinary research*. 2016;47(1):1-19. [PMID: 27894330] [PMCID: PMC5127044] <https://doi.org/10.1186/s13567-016-0404-3>
3. Biggs PM, Nair V. The long view: 40 years of Marek's disease research and Avian Pathology. *Avian pathology*. 2012;41(1):3-9. [PMID: 22845316] <https://doi.org/10.1080/03079457.2011.646238>
4. Marek J. Multiple Nerventzündung (Polyneuritis) bei Hühnern. *Dtsch Tierarztl Wochenschr*. 1907;15:417-521.
5. Rispens BH, van Vloten H, Mastenbroek N, Maas HJ, Schat KA. Control of Marek's disease in the Netherlands. I. Isolation of an avirulent Marek's disease virus (strain CVI 988) and its use in laboratory vaccination trials. *Avian diseases*. 1972;108-25. [PMID: 4337307] <https://doi.org/10.2307/1588905>
6. Rispens BH, van Vloten H, Mastenbroek N, Maas HJ, Schat KA. Control of Marek's disease in the Netherlands. II. Field trials on vaccination with an avirulent strain (CVI 988) of Marek's disease virus. *Avian diseases*. 1972;126-38. [PMID: 4337309] <https://doi.org/10.2307/1588906>
7. Vielitz E, Landgraf H. Prevention of Marek's disease by various vaccination viruses following test infection at various ages, study of PD50. *DTW Deutsche Tierärztliche Wochenschrift*. 1986;93(1):53-6. [PMID: 3009131]
8. Witter R, editor Safety and comparative efficacy of the CVI988/Rispens vaccine strain. 4th International Symposium on Marek's Disease, 19th World's Poultry Congress; 1992: World's Poultry Science Association Amsterdam, the Netherlands.
9. Gimeno IM, Faiz NM, Cortes AL, Barbosa T, Villalobos T, Pandiri AR. In ovo vaccination with turkey herpesvirus hastens maturation of chicken embryo immune responses in specific-pathogen-free chickens. *Avian diseases*. 2015;59(3):375-83. [PMID: 26478155] <https://doi.org/10.1637/11060-031115-reg.1>
10. Shah AU, Wang Z, Zheng Y, Guo R, Chen S, Xu M, et al. Construction of a Novel Infectious Clone of Recombinant Herpesvirus of Turkey Fc-126 Expressing VP2 of IBDV. *Vaccines*. 2022;10(9):1391. [PMID: 27388394] <https://doi.org/10.12968/hmed.2016.77.7.c98>
11. Landman WJM, Verschuren SBE. Titration of Marek's disease cell-associated vaccine virus (CVI 988) of reconstituted vaccine and vaccine ampoules from Dutch hatcheries. *Avian Diseases*. 2003;47(4):1458-65. [PMID: 14708997] <https://doi.org/10.1637/7034>
12. Savage HM, Burkhalter KL, Godsey Jr MS, Panella NA, Ashley DC, Nicholson WL, Lambert AJ. Bourbon virus in field-collected ticks, Missouri, USA. *Emerging Infectious Diseases*. 2017;23(12).
13. Schaible UE, Kaufmann SH. 19 Studying trafficking of intracellular pathogens in antigen-presenting cells. *Methods in Microbiology*. 2002;31:343-60. [https://doi.org/10.1016/s0580-9517\(02\)31020-1](https://doi.org/10.1016/s0580-9517(02)31020-1)
14. Baer A, Kehn-Hall K. Viral concentration determination through plaque assays: using traditional and novel overlay systems. *JoVE (Journal of Visualized Experiments)*. 2014(93):e52065. [PMID: 25407402] [PMCID: PMC4255882] <https://doi.org/10.3791/52065-v>
15. King C. Department of Mathematics University of Auckland, New Zealand Genotype 1.1. 18 1978 Aug 2016 PDF.
16. Yakimovich A, Andriasyan V, Witte R, Wang I-H, Prasad V, Suomalainen M, Greber UF. Plaque2. 0—a high-throughput analysis framework to score virus-cell transmission and clonal cell expansion. *PLoS one*. 2015;10(9):e0138760. [PMID: 26413745] [PMCID: PMC4587671] <https://doi.org/10.1371/journal.pone.0138760>
17. Flint SJ, Racaniello VR, Rall GF, Hatzioannou T, Skalka AM. Principles of virology, Volume 2: pathogenesis and control: John Wiley & Sons; 2020. <https://doi.org/10.1128/9781555818968>
18. Barreca C, O'Hare P. Suppression of herpes simplex virus 1 in MDBK cells via the interferon pathway. *Journal of virology*. 2004;78(16):8641-53. [PMID: 15280473] [PMCID: PMC479083] <https://doi.org/10.1128/jvi.78.16.8641-8653.2004>
19. Barreca 2004.
20. Ackermann-Gäumann R, Siegrist D, Züst R, Signer J, Lenz N, Engler O. Standardized focus assay protocol for biosafety level four viruses. *Journal of virological methods*. 2019;264:51-4. [PMID: 30513365] <https://doi.org/10.1016/j.jviromet.2018.12.002>
21. Lindenbach BD. Measuring HCV infectivity produced in cell culture and in vivo. *Hepatitis C: methods and protocols*. 2009:329-36. [PMID: 19009272] https://doi.org/10.1007/978-1-59745-394-3_24
22. Payne S. *Viruses*: Academic Press Cambridge, MA, USA.; 2017.
23. Khoury DS, Wheatley AK, Ramuta MD, Reynaldi A, Cromer D, Subbarao K, et al. Measuring immunity to SARS-CoV-2 infection: comparing assays and animal models. *Nature Reviews Immunology*. 2020;20(12):727-38. [PMID: 33139888] [PMCID: PMC7605490] <https://doi.org/10.1038/s41577-020-00471-1>
24. Kärber G. Beitrag zur kollektiven Behandlung pharmakologischer Reihenversuche. *Naunyn-Schmiedebergs Archiv für experimentelle pathologie und pharmakologie*. 1931;162:480-3. <https://doi.org/10.1007/bf01863914>
25. Killian ML. Hemagglutination assay for the avian influenza virus. *Avian influenza virus*. 2008:47-52. [PMID: 18370040] https://doi.org/10.1007/978-1-59745-279-3_7
26. Rimmelzwaan G, Baars M, Claas E, Osterhaus A. Comparison of RNA hybridization, hemagglutination assay, titration of infectious virus and immunofluorescence as methods for monitoring influenza virus replication in vitro. *Journal of virological methods*. 1998;74(1):57-66. [PMID: 9763129] [https://doi.org/10.1016/s0166-0934\(98\)00071-8](https://doi.org/10.1016/s0166-0934(98)00071-8)

27. Kato A, Kiyotani K, Sakai Y, Yoshida T, Nagai Y. The paramyxovirus, Sendai virus, V protein encodes a luxury function required for viral pathogenesis. *The EMBO journal*. 1997;16(3):578-87. [PMID: 9034340] [PMCID: PMC1169661] <https://doi.org/10.1093/emboj/16.3.578>
28. Jonges M, Liu WM, van der Vries E, Jacobi R, Pronk I, Boog C, et al. Influenza virus inactivation for studies of antigenicity and phenotypic neuraminidase inhibitor resistance profiling. *Journal of clinical microbiology*. 2010;48(3):928-40. [PMID: 20089763] [PMCID: PMC2832438] <https://doi.org/10.1128/jcm.02045-09>
29. Wędrowska E, Wandtke T, Piskorska E, Kopiński P. The latest achievements in the construction of influenza virus detection aptasensors. *Viruses*. 2020;12(12):1365.
30. Khodayari M, Feizi A. Evaluation of different routes of vaccination by clone vaccine on humoral antibody response. *Exploratory Animal and Medical Research*. 2017;7(2):165-9.
31. Hancock K, Veguilla V, Lu X, Zhong W, Butler EN, Sun H, et al. Cross-reactive antibody responses to the 2009 pandemic H1N1 influenza virus. *New England journal of medicine*. 2009;361(20):1945-52. <https://doi.org/10.1056/nejmoa0906453>
32. Vasfi MM, BOZORG MM. Isolation of H9N2 subtype of avian influenza viruses during an outbreak in chickens in Iran. 2002.
33. Fereidouni S, Bozorghmehrfard M, Starick E, Werner O, Amini H, Modirrousta H, Aghakhan M. Serological monitoring of avian influenza in migratory birds of Iran. *Archives of Razi Institute*. 2005;60(1):11-20. <https://doi.org/10.1136/vr.157.17.526>.
34. Olson BJ, Markwell J. Assays for determination of protein concentration. *Current protocols in protein science*. 2007;48(1):3.4. 1-3.4. 29. [PMID: 18429326] <https://doi.org/10.1002/0471140864.ps0304s48>.
35. Wiechelmann KJ, Braun RD, Fitzpatrick JD. Investigation of the bicinchoninic acid protein assay: identification of the groups responsible for color formation. *Analytical biochemistry*. 1988;175(1):231-7. [PMID: 3245570] [https://doi.org/10.1016/0003-2697\(88\)90383-1](https://doi.org/10.1016/0003-2697(88)90383-1)
36. Smith Pe, Krohn RI, Hermanson G, Mallia A, Gartner F, Provenzano M, et al. Measurement of protein using bicinchoninic acid. *Analytical biochemistry*. 1985;150(1):76-85. [PMID: 3843705] [https://doi.org/10.1016/0003-2697\(85\)90442-7](https://doi.org/10.1016/0003-2697(85)90442-7)
37. Rich RR, Fleisher TA, Shearer WT, Schroeder Jr HW, Frew AJ, Weyand CM. *Clinical immunology e-book: principles and practice*: Elsevier Health Sciences; 2012.
38. Rodda SJ, Gallichio HA, Hampson AW. The single radial immunodiffusion assay highlights small antigenic differences among influenza virus hemagglutinins. *Journal of clinical microbiology*. 1981;14(5):479-82. [PMID: 6171580] <https://doi.org/10.1128/jcm.14.5.479-482.1981>
39. Williams TL, Pirkle JL, Barr JR. Simultaneous quantification of hemagglutinin and neuraminidase of influenza virus using isotope dilution mass spectrometry. *Vaccine*. 2012;30(14):2475-82. [PMID: 22197963] <https://doi.org/10.1016/j.vaccine.2011.12.056>
40. Dykstra MJ, Reuss LE. *Biological electron microscopy: theory, techniques, and troubleshooting*: Springer Science & Business Media; 2011.
41. Cheville N, Stasko J. Techniques in electron microscopy of animal tissue. *Veterinary pathology*. 2014;51(1):28-41. [PMID: 24114311] <https://doi.org/10.1177/0300985813505114>
42. Mast J, Demeestere L. Electron tomography of negatively stained complex viruses: application in their diagnosis. *Diagnostic Pathology*. 2009;4(1):1-7. [PMID: 19208223] [PMCID: PMC2649040] <https://doi.org/10.1186/1746-1596-4-5>
43. Richert-Pöggeler KR, Franzke K, Hipp K, Kleespies RG. Electron microscopy methods for virus diagnosis and high resolution analysis of viruses. *Frontiers in microbiology*. 2019;9:3255. [PMID: 30666247] [PMCID: PMC6330349] <https://doi.org/10.3389/fmicb.2018.03255>
44. Blancett CD, Fetterer DP, Koistinen KA, Morazzani EM, Monninger MK, Piper AE, et al. Accurate virus quantitation using a Scanning Transmission Electron Microscopy (STEM) detector in a scanning electron microscope. *Journal of virological methods*. 2017;248:136-44. [PMID: 28668710] <https://doi.org/10.1016/j.jviromet.2017.06.014>
45. Hayat M, Miller S. *Negative Staining* McGraw. Hill Publishing Co., New York, NY; 1990.
46. Skevaki CL, Papadopoulos NG, Tsakris A, Johnston SL. Microbiologic diagnosis of respiratory illness: practical applications. *Kendig & Chernick's Disorders of the Respiratory Tract in Children*. 2012:399.
47. Sowerby SJ, Broom MF, Petersen GB. Dynamically resizable nanometre-scale apertures for molecular sensing. *Sensors and Actuators B: Chemical*. 2007;123(1):325-30. <https://doi.org/10.1016/j.snb.2006.08.031>
48. Roberts GS, Yu S, Zeng Q, Chan LC, Anderson W, Colby AH, et al. Tunable pores for measuring concentrations of synthetic and biological nanoparticle dispersions. *Biosensors and Bioelectronics*. 2012;31(1):17-25.
49. C.D. Humphrey 2021. [PMID: 22019099] <https://doi.org/10.1016/j.bios.2011.09.040>
50. Yang L, Yamamoto T. Quantification of virus particles using nanopore-based resistive-pulse sensing techniques. *Frontiers in microbiology*. 2016;7:1500. [PMID: 27713738] [PMCID: PMC5031608] <https://doi.org/10.3389/fmicb.2016.01500>
51. Rieseberg M, Kasper C, Reardon KF, Scheper T. Flow cytometry in biotechnology. *Applied microbiology and biotechnology*. 2001;56:350-60. [PMID: 11549001] <https://doi.org/10.1007/s002530100673>
52. Zamora JLR, Aguilar HC. Flow virometry as a tool to study viruses. *Methods*. 2018;134:87-97. [PMID: 11549001] <https://doi.org/10.1016/j.ymeth.2017.12.011>
53. Van Der Pol E, Hoekstra A, Sturk A, Otto C, Van Leeuwen T, Nieuwland R. Optical and non-optical methods for detection and characterization of microparticles and exosomes. *Journal of Thrombosis and Haemostasis*. 2010;8(12):2596-607. [PMID: 20880256] <https://doi.org/10.1111/j.1538-7836.2010.04074.x>
54. Wang Y, Hammes F, De Roy K, Verstraete W, Boon N. Past, present and future applications of flow cytometry in aquatic microbiology. *Trends in biotechnology*. 2010;28(8):416-24. [PMID: 20541271] <https://doi.org/10.1016/j.tibtech.2010.04.006>
55. Hercher M, Mueller W, Shapiro HM. Detection and discrimination of individual viruses by flow cytometry. *Journal of Histochemistry & Cytochemistry*. 1979;27(1):350-2. [PMID: 374599] <https://doi.org/10.1177/27.1.374599>
56. Brussaard CP, Marie D, Bratbak G. Flow cytometric detection of viruses. *Journal of virological methods*. 2000;85(1-2):175-82. [PMID: 10716350] [https://doi.org/10.1016/s0166-0934\(99\)00167-6](https://doi.org/10.1016/s0166-0934(99)00167-6)
57. Stoffel CL, Rowlen KL. Data analysis for a dual-channel virus counter. *Analytical Chemistry*. 2005;77(7):2243-6. [PMID: 15830378]

58. Degueldre C, Favarger P-Y, Bitea C. Zirconia colloid analysis by single particle inductively coupled plasma–mass spectrometry. *Analytica Chimica Acta*. 2004;518(1-2):137-42. [https://doi.org/10.1016/s0927-7757\(02\)00568-x](https://doi.org/10.1016/s0927-7757(02)00568-x)
59. Degueldre C, Favarger P-Y, Wold S. Gold colloid analysis by inductively coupled plasma-mass spectrometry in a single particle mode. *Analytica Chimica Acta*. 2006;555(2):263-8. <https://doi.org/10.1016/j.aca.2005.09.021>
60. de Jesus JR, de Araújo Andrade T. Understanding the relationship between viral infections and trace elements from a metallomics perspective: implications for COVID-19. *Metallomics*. 2020;12(12):1912-30.
61. Laborda F, Bolea E, Jimenez-Lamana J. Single particle inductively coupled plasma mass spectrometry: a powerful tool for nanoanalysis. ACS Publications; 2014. [PMID: 24308527] <https://doi.org/10.1021/ac402980q>
62. Wilschefski SC, Baxter MR. Inductively coupled plasma mass spectrometry: introduction to analytical aspects. *The Clinical Biochemist Reviews*. 2019;40(3):115. [PMID: 31530963] [PMCID: PMC6719745] <https://doi.org/10.33176/aacb-19-00024>
63. Degueldre C. Single virus inductively coupled plasma mass spectroscopy analysis: A comprehensive study. *Talanta*. 2021;228:122211. [PMID: 33773712] <https://doi.org/10.1016/j.talanta.2021.122211>
64. Botes M, de Kwaadsteniet M, Cloete TE. Application of quantitative PCR for the detection of microorganisms in water. *Analytical and bioanalytical chemistry*. 2013;405:91-108. [PMID: 23001336] [PMCID: PMC7079929] <https://doi.org/10.1007/s00216-012-6399-3>
65. Engstrom-Melnik J, Rodriguez PL, Peraud O, Hein RC. Clinical applications of quantitative real-time PCR in virology. *Methods in Microbiology*. 42: Elsevier; 2015. p. 161-97. <https://doi.org/10.1016/bs.mim.2015.04.005>
66. Tajadini M, Panjehpour M, Javanmard SH. Comparison of SYBR Green and TaqMan methods in quantitative real-time polymerase chain reaction analysis of four adenosine receptor subtypes. *Advanced biomedical research*. 2014;3. <https://doi.org/10.4103/2277-9175.127998>
67. Wang L, Blasic Jr J, Holden M, Pires R. Sensitivity comparison of real-time PCR probe designs on a model DNA plasmid. *Analytical biochemistry*. 2005;344(2):257-65. [PMID: 16091278] <https://doi.org/10.1016/j.ab.2005.06.038>
68. Lemmon GH, Gardner SN. Predicting the sensitivity and specificity of published real-time PCR assays. *Annals of clinical microbiology and antimicrobials*. 2008;7(1):1-10. [PMID: 18817537] [PMCID: PMC2566554] <https://doi.org/10.1186/1476-0711-7-18>
69. O'Leary JJ, Sheils O, Martin C, Crowley A. TaqMan Technology and Real-Time Polymerase Chain Reaction. *Molecular biology in cellular pathology*. 2003;251. <https://doi.org/10.1002/0470867949.ch12>
70. Smith CJ, Osborn AM. Advantages and limitations of quantitative PCR (Q-PCR)-based approaches in microbial ecology. *FEMS microbiology ecology*. 2009;67(1):6-20. [PMID: 19120456] <https://doi.org/10.1111/j.1574-6941.2008.00629.x>
71. Shah K, Maghsoudlou P. Enzyme-linked immunosorbent assay (ELISA): the basics. *British journal of hospital medicine*. 2016;77(7):C98-C101. [PMID: 27388394] <https://doi.org/10.12968/hmed.2016.77.7.c98>
72. MacGillivray A. ELISA and other solid phase immunoassays: Theoretical and practical aspects: Edited by DM Kemeny and SJ Challacombe John Wiley & Sons, Chichester, 1988 367 pages.£ 24.95. Wiley Online Library; 1989.
73. Kindt TJ, Goldsby RA, Osborne BA, Kuby J. Kuby immunology: Macmillan; 2007.
74. Aydin S. A short history, principles, and types of ELISA, and our laboratory experience with peptide/protein analyses using ELISA. *Peptides*. 2015;72:4-15. [PMID: 25908411] <https://doi.org/10.1016/j.peptides.2015.04.012>
75. Alexander I, Ashley C, Smith K, Harbour J, Roome A, Darville J. Comparison of ELISA with virus isolation for the diagnosis of genital herpes. *Journal of clinical pathology*. 1985;38(5):554-7. [PMID: 2987313] [PMCID: PMC499207] <https://doi.org/10.1136/jcp.38.5.554>
76. Mohammadi A, Keyvanfar H, Hematzadeh F, BOZORG MM. Molecular diagnosis of Marek's disease virus (MDV) in Iran. 2005.
77. Schat K. Isolation of Marek's disease virus: revisited. *Avian Pathology*. 2005;34(2):91-5.
78. Aydin S. A short history, principles, and types of ELISA, and our laboratory experience with peptide/protein analyses using ELISA. *Peptides*. 2015 Oct 1;72:4-15. [PMID: 25908411] <https://doi.org/10.1016/j.peptides.2015.04.012>
79. Schat K. Characteristics of the virus. Marek's disease: scientific basis and methods of control: Springer; 1985. p. 77-112. [PMID: 16191687] <https://doi.org/10.1080/03079450500059289>
80. Witter R. Characteristics of Marek's disease viruses isolated from vaccinated commercial chicken flocks: association of viral pathotype with lymphoma frequency. *Avian Diseases*. 1983;113-32. [PMID: 6303287] <https://doi.org/10.2307/1590377>
81. Calnek B, Shek W, Schat K, Fabricant J. Dose-dependent inhibition of virus rescue from lymphocytes latently infected with turkey herpesvirus or Marek's disease virus. *Avian Diseases*. 1982;321-31. [PMID: 6285880] <https://doi.org/10.2307/1590101>
82. Witter R, Solomon J, Burgoyne G. Cell culture techniques for primary isolation of Marek's disease-associated herpesvirus. *Avian Diseases*. 1969:101-18. [PMID: 6303287] <https://doi.org/10.2307/1590377>